

## Temperature Dependent Rate Coefficient for the Cl + ClONO<sub>2</sub> Reaction

R. J. Yokelson,<sup>†</sup> James B. Burkholder,\* Leah Goldfarb,<sup>‡</sup> R. W. Fox,<sup>§</sup> Mary K. Gilles, and A. R. Ravishankara<sup>‡</sup>

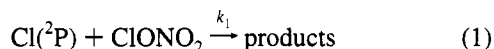
Aeronomy Laboratory, NOAA, 325 Broadway, Boulder, Colorado 80303, and The Cooperative Institute for Research in Environmental Sciences, University of Colorado, Boulder, Colorado 80309

Received: April 17, 1995<sup>⊗</sup>

The rate coefficient for reaction 1, Cl + ClONO<sub>2</sub> → products was measured between 195 and 354 K. Cl atoms were generated by pulsed laser photolysis of Cl<sub>2</sub> in an excess of ClONO<sub>2</sub>. The temporal profiles of Cl atom loss and NO<sub>3</sub> product formation were monitored using resonance fluorescence and tunable diode laser absorption at 662 nm, respectively. The long path absorption system was used to measure *k*<sub>1</sub> between 200 and 298 K while the resonance fluorescence system was employed between 195 and 354 K. Thermal decomposition of ClONO<sub>2</sub> prevented measurements at temperatures greater than 354 K. The two techniques yielded rate coefficients which are in excellent agreement. An Arrhenius rate coefficient expression of *k*<sub>1</sub> = (6.0 ± 0.4) × 10<sup>-12</sup> exp[(140 ± 30)/*T*] cm<sup>3</sup> molecule<sup>-1</sup> s<sup>-1</sup> and room temperature rate constant of *k*<sub>1</sub>(298 K) = (9.6 ± 1.0) × 10<sup>-12</sup> cm<sup>3</sup> molecule<sup>-1</sup> s<sup>-1</sup> were derived from data at *T* ≤ 298 K. The quoted error limits are 2σ and include estimated systematic errors. Our results are compared with previous measurements, and values of *k*<sub>1</sub> for atmospheric modeling are recommended.

### Introduction

Chlorine nitrate, ClONO<sub>2</sub>, is an important reservoir for chlorine in the stratosphere. Its abundance can be as much as 50% of the inorganic chlorine, i.e., chlorine-containing species produced from the atmospheric degradation of organic chlorine compounds.<sup>1–3</sup> Any process that converts ClONO<sub>2</sub> to forms that can engage in catalytic ozone destruction cycles, such as Cl and ClO, is of importance to stratospheric chemistry. The major processes that convert ClONO<sub>2</sub> to active forms are believed to be its photolysis and heterogeneous reactions. The photolysis lifetime of ClONO<sub>2</sub> is on the order of a few hours in the midlatitude stratosphere.<sup>4</sup> The rates of the heterogeneous processes are very dependent on temperature and the presence of suitable condensed matter to provide a surface for the reactions. The lifetime of ClONO<sub>2</sub> due to the heterogeneous processes can be as short as a couple of days in the presence of certain polar stratospheric clouds to as long as many years in warm midlatitudes under background sulfate aerosol loading. Reaction of ClONO<sub>2</sub> with free radicals such as O(<sup>3</sup>P), Cl(<sup>2</sup>P), and OH plays a smaller role than photolysis. The lifetime of ClONO<sub>2</sub> due to its reaction with Cl atoms,



can be tens of hours, depending on the Cl atom concentration, which changes with factors such as solar zenith angle, temperature, and abundance of other stratospheric constituents. Yet, this reaction is not negligible and should be considered for a complete understanding of the stratosphere. Further, this reaction is often used in the laboratory for the production of NO<sub>3</sub> and may be unavoidable when ClONO<sub>2</sub> is present.

Therefore, accurate values of *k*<sub>1</sub> as a function of temperature are useful for designing, controlling, and evaluating laboratory studies.

Originally reaction 1 was reported to be quite slow, similar to the reaction of OH with ClONO<sub>2</sub>.<sup>5,6</sup> In the early 1980's it was discovered by Margitan<sup>7</sup> and confirmed by Kurylo *et al.*,<sup>8</sup> that this reaction is quite rapid. The value of *k*<sub>1</sub> measured by Margitan and Kurylo *et al.* agrees to within 20% with an average value of *k*<sub>1</sub> = 1.15 × 10<sup>-11</sup> cm<sup>3</sup> molecule<sup>-1</sup> s<sup>-1</sup> at 298 K. Both studies, on whose results the current recommendations<sup>9,10</sup> are based, used similar techniques.

We recently undertook the study of the photochemistry of ClONO<sub>2</sub>. During this study, reaction 1 played a major role, since Cl atoms were always produced as photodissociation products. Therefore, we carried out a comprehensive study of this reaction as a function of temperature. The results are presented in this paper. The rate coefficient *k*<sub>1</sub> was measured by observing the formation of NO<sub>3</sub> product, using transient visible absorption, and the loss of Cl atom reactant, using atomic resonance fluorescence, over the temperature range 195–354 K. In this paper, we compare our measured values of *k*<sub>1</sub> with those from previous measurements and report a recommended value for use in atmospheric model calculations.

### Experimental Details

The rate coefficient *k*<sub>1</sub> was measured using two different apparatus. In both apparatus, Cl atoms were produced by pulsed photolysis of Cl<sub>2</sub> in an excess of ClONO<sub>2</sub>. In the resonance fluorescence apparatus, the removal of Cl atoms was monitored by vacuum UV atomic resonance fluorescence. In the long path absorption apparatus, the temporal evolution of the NO<sub>3</sub> product was monitored via diode laser absorption at 662 nm. These two experimental approaches are complementary and serve to identify and reduce possible systematic errors in measuring the rate coefficient. Details of the laser photolysis–time-resolved absorption apparatus were described by Yokelson *et al.*<sup>11</sup> The resonance fluorescence apparatus, which has been used in a number of kinetic and quantum yield studies in our laboratory, has been described elsewhere.<sup>12,13</sup> Therefore, only the specifics relevant to the current measurements of *k*<sub>1</sub> are presented below.

\* Author to whom correspondence should be sent: NOAA R/E/AL2, 325 Broadway, Boulder, CO 80303.

<sup>†</sup> Present address: Department of Chemistry, University of Montana, Missoula, MT 59812.

<sup>‡</sup> Also affiliated with the Department of Chemistry and Biochemistry, University of Colorado, Boulder, CO 80309.

<sup>§</sup> National Institute for Standards and Technology, Time and Frequency Division, 325 Broadway, Boulder, CO 80303.

<sup>⊗</sup> Abstract published in *Advance ACS Abstracts*, September 1, 1995.

**Transient Absorption Measurements.** The apparatus consisted of four basic components: (1) a reactor, which is a single pass jacketed absorption cell with an optical path length of 91 cm, (2) a pulsed XeF (351 nm) excimer laser, which is the photolysis light source, (3) a tunable visible diode laser, and (4) a detector for measuring the intensity of the tunable visible diode laser. The jacketed absorption cell was made of 30-mm-i.d. Pyrex tubing. The temperature was regulated by circulating methanol from a temperature-controlled bath through the jacket. The temperature over the length of the absorption cell was constant to  $\pm 1$  K. The concentrations of the ClONO<sub>2</sub> and Cl<sub>2</sub> flowing through the absorption cell were measured in situ using a D<sub>2</sub> lamp light source and a 0.28 m spectrograph equipped with a diode array detector. Absorptions in the wavelength range 200–380 nm were recorded. Even though both ClONO<sub>2</sub> and Cl<sub>2</sub> have unstructured absorption spectra, because of the differences in their absorption spectra, both these species could be quantified using this wavelength range. The linear flow velocities in the absorption cell were in the range 6–15 cm s<sup>-1</sup>, such that the reactor was completely replenished with a fresh reaction mixture between laser pulses.

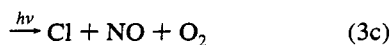
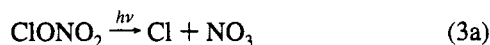
The laser photolysis beam and the probe beams were copropagated along the length of the absorption cell. Either the diode laser or D<sub>2</sub> lamp beam was passed through the absorption cell at a given time. Positive position mounted mirrors allowed quick and reproducible switching between the two beams and their detectors. The 662 nm tunable diode laser beam was detected by a photodiode.

The diode laser, with a nominal wavelength of 662 nm, ran single mode with an output power between 0.5 and 2 mW. This beam was used to measure NO<sub>3</sub> transient absorption signals. The nominal wavelength of the diode laser ( $\pm 0.1$  nm) was measured using the diode array system. The laser wavelength was locked at the peak of the NO<sub>3</sub> absorption feature, 661.9 nm, by regulating the laser current ( $\sim 40$  mA) and temperature ( $\sim 275$  K). The exact wavelength of the diode laser need not be known for the rate coefficient measurements; the reaction is first order in Cl atom loss and NO<sub>3</sub> production, and hence, a knowledge of the absolute concentrations of NO<sub>3</sub> is not needed. However, the concentration of NO<sub>3</sub> produced was needed for estimating the influence of secondary reactions. The detection limit, based on our absorption sensitivity, for NO<sub>3</sub> in this system was  $\sim 2 \times 10^{10}$  molecule cm<sup>-3</sup> for a single photolysis laser shot.

A XeF excimer laser (351 nm) was used to photolyze Cl<sub>2</sub> and generate Cl atoms,



In addition to Cl<sub>2</sub>, ClONO<sub>2</sub> can also be photolyzed and contribute to the production of Cl atoms,



However, because of the small absorption cross section for ClONO<sub>2</sub> at 351 nm and the relatively larger concentrations of Cl<sub>2</sub> that were used, the concentration of Cl atoms produced from reaction 3 was negligible compared to that from reaction 2. The Cl atoms produced from reaction 3 was calculated to be very

small and confirmed by photolyzing only ClONO<sub>2</sub> and observing a negligibly small NO<sub>3</sub> signal. Thus, the concentration of NO<sub>3</sub> produced was accurately reflected by that of Cl atoms produced solely by the photolysis of Cl<sub>2</sub>.

In a given experiment, a mixture of Cl<sub>2</sub> and ClONO<sub>2</sub> in a large abundance (50 to 500 Torr) of He or N<sub>2</sub> was flowed through the reactor. The concentrations of Cl<sub>2</sub> and ClONO<sub>2</sub> were measured using the D<sub>2</sub> lamp and the diode array spectrometer. Following this measurement, the D<sub>2</sub> lamp was replaced by the 662 nm diode laser beam. The intensity of the laser beam was monitored for  $\sim 1$  ms, and then the photolysis excimer laser was fired. The temporal profile of the 662 nm beam was monitored for at least 10 ms after the laser pulse. Using the intensity of the diode laser before the excimer pulse as  $I_0$ , the post photolysis absorbance temporal profile was calculated. This absorption profile was analyzed to obtain the rate coefficient for the loss of Cl atoms at that [ClONO<sub>2</sub>]. Such profiles were measured at various concentrations of ClONO<sub>2</sub> at 298, 258, 230, and 200 K.

**Cl Atom Resonance Fluorescence.** Chlorine atoms were produced via photolysis of Cl<sub>2</sub> at 355 nm (third harmonic of a Nd:YAG laser). A mixture of N<sub>2</sub>O and N<sub>2</sub> was used to flush the space between the photomultiplier tube and the reactor. The flow of N<sub>2</sub>O was adjusted such that all the signal from O(<sup>3</sup>P), produced by 248 nm photolysis of an O<sub>3</sub>/N<sub>2</sub> mixture, was eliminated. This amount of N<sub>2</sub>O reduced the Cl atom signal by less than 10%. N<sub>2</sub>O absorbs the resonance radiation from O atoms very strongly, while passing the majority of Cl atom radiation. This filter prevents inadvertent detection of O atoms in the Cl atom experiments. (Note: it is suspected that interference from O atom detection was one of the possible reasons for the earlier measurements<sup>5,6</sup> being erroneous!) In addition, we also mounted a CaF<sub>2</sub> window in front of the PMT to eliminate the detection of Lyman- $\alpha$  radiation at 121.6 nm. Thus only Cl atoms were detected during this experiment. Under these operating conditions, the sensitivity for Cl atom detection in 100 Torr of He was typically  $3 \times 10^7$  cm<sup>-3</sup> for a 1 s integration time.

A mixture of ClONO<sub>2</sub> in He was prepared in a 12 L glass bulb. This mixture was flowed through a 100 cm long absorption cell, where the concentration of ClONO<sub>2</sub> was directly measured via absorption at 213.9 nm (zinc lamp,  $\sigma = 3.39 \times 10^{-18}$  cm<sup>2</sup> molecule<sup>-1</sup>). This mixture of ClONO<sub>2</sub> in He was diluted in the reactor by adding more He. The extent of dilution was obtained from the measured flow rates and the pressures in the reactor and the absorption cells. The flow rates and pressures were measured using calibrated electronic flow meters and capacitance manometers, respectively. To ensure that our dilution was accurate, we carried out similar dilution of an O<sub>3</sub>/He mixture but measured the concentration of O<sub>3</sub> in the original mixture (at 213.9 nm) as well as in the diluted mixture (at 253.7 nm). The final concentrations of O<sub>3</sub> measured via absorption and deduced from measured flow rates were the same to within 2%. This test gives us confidence in our measured concentrations of ClONO<sub>2</sub>, which varied from  $9 \times 10^{12}$  to  $1.7 \times 10^{14}$  molecule cm<sup>-3</sup> in the reactor. The ClONO<sub>2</sub> concentrations in the reactor at  $T \approx 298$  K were calculated from the concentrations determined at 298 K and the known temperature of the reactor. In a few experiments, where high concentrations of ClONO<sub>2</sub> were used, the concentration of ClONO<sub>2</sub> in the mixture flowing through the reactor was measured directly via UV absorption; the measured  $k_1$  values were the same as those using the dilution method.

In a typical experiment, a mixture of Cl<sub>2</sub> and ClONO<sub>2</sub> in He was photolyzed by 355 nm radiation from a Nd:YAG laser. The Cl atom temporal profiles were coadded 100–2000 times

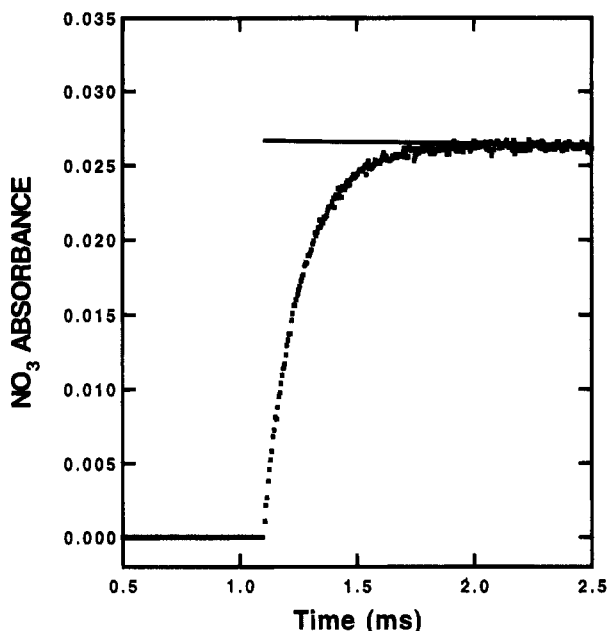


**Figure 1.** Temporal profile of the  $\text{NO}_3$  absorption signal following laser photolysis, 351 nm, of a  $\text{Cl}_2/\text{ClONO}_2$  mixture. The solid line was obtained by fitting the data at time  $> 0.002$  s to a first-order loss of  $\text{NO}_3$ . This line was extrapolated to  $t_0$  (when photolysis laser fired), where the absorbance is  $A_\infty$ , and used in the data analysis using eq 4.

to enhance the signal to noise ratio. Such averaged profiles were measured at various concentrations of  $\text{ClONO}_2$  to extract the value of  $k_1$ . These measurements were repeated at 10 temperatures in the range 195–354 K.

**Materials.**  $\text{ClONO}_2$  was synthesized by the reaction of  $\text{Cl}_2\text{O}$  with  $\text{N}_2\text{O}_5$ ,<sup>4</sup> stored in the dark at 195 K, and introduced into the apparatus with a flow of He, which was dried by passing it through a molecular sieve trap at 77 K. The only impurity we could detect in our sample of  $\text{ClONO}_2$  by UV absorption was  $\text{OCIO}$ . Its fractional concentration in  $\text{ClONO}_2$  was always  $\leq 0.006\%$ . In our purified samples of  $\text{ClONO}_2$ , we could not detect any  $\text{NO}_2$  via UV absorption; therefore, we estimate its fractional concentration to be  $< 0.06\%$ . The  $\text{ClONO}_2$  samples were also analyzed by chemical ionization mass spectrometry to quantify the levels of  $\text{Cl}_2$  and  $\text{Cl}_2\text{O}$ ; their fractional levels were determined to be  $< 0.2\%$  and  $0.1\%$ , respectively.  $\text{O}_3$  was prepared with a commercial ozonizer and stored on silica gel at 195 K and introduced to the absorption cell with a flow of  $\text{N}_2$ .  $\text{N}_2$  (UHP,  $> 99.9995\%$ ) was used as supplied. A mixture of chlorine in He (electronic grade, 1000 ppmv  $\text{Cl}_2$  in He which was  $> 99.97\%$  pure) was used as supplied.  $\text{N}_2\text{O}$  (99.99%) and  $\text{N}_2$  (99.98%) were used for flush gases. In the resonance fluorescence apparatus, helium (UHP,  $> 99.999\%$ ) gas to the resonance lamp was passed through a liquid nitrogen trap before use.  $\text{CF}_4$  (99.965%), used for quenching  $\text{Cl}(^2\text{P}_{1/2})$ , was purified with repeated freeze/pump/thaw cycles to remove  $\text{O}_2$ .

## Results

The data acquisition and analysis procedures used in the two apparatus are different. Therefore the results from the two different sets of measurements are presented separately.

**Transient Absorption Measurements.** Figure 1 shows a typical temporal profile of the  $\text{NO}_3$  absorption signal measured at 662 nm following the XeF, 351 nm, laser photolysis of a mixture of  $\text{Cl}_2/\text{ClONO}_2/\text{He}$ . Meaningful absorbance measurements at reaction times less than  $\sim 20$   $\mu\text{s}$  were not possible due to scattered light from the photolysis laser reaching the detector. This temporal profile clearly shows the formation of  $\text{NO}_3$  via

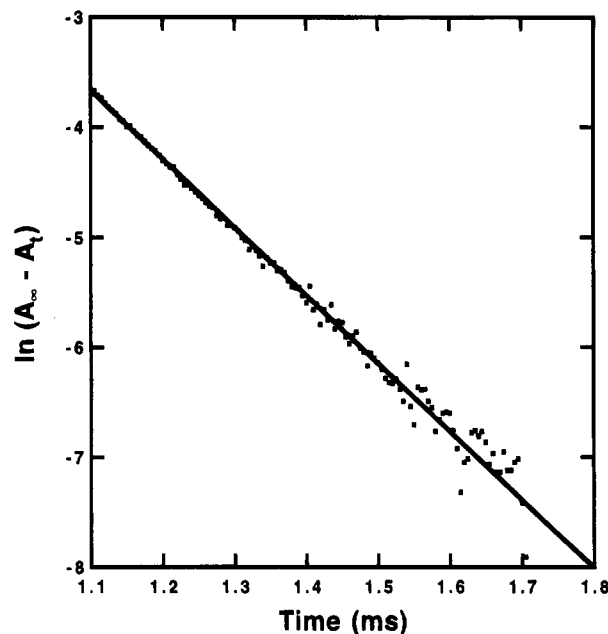


**Figure 2.** Typical kinetic analysis of the  $\text{NO}_3$  absorption signal to obtain the first-order rate coefficient for reaction 1 in excess  $\text{ClONO}_2$ . The data are the same as those shown in Figure 1. The solid line is the least squares fit to the data. The conditions of this measurement were  $T = 200$  K,  $[\text{ClONO}_2] = 5.79 \times 10^{14}$  molecule  $\text{cm}^{-3}$ , and  $[\text{ClONO}_2]/[\text{Cl}]_0 = 64.7$ .

reaction 1. Also, the concentration of  $\text{NO}_3$  was zero right after the photolysis laser fired, implying that the amount of  $\text{NO}_3$  produced by the photolysis of  $\text{ClONO}_2$  was insignificant.

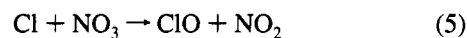
The temporal profiles of transmitted light intensity were converted to time dependent absorptions using the light intensity prior to the laser pulse as  $I_0$ . The calculated temporal profiles of the absorbances follow the equation

$$\ln(A_\infty - A_t) - k_1[\text{ClONO}_2]t = k_1't \quad (4)$$

where  $A_\infty$  is the  $\text{NO}_3$  absorbance at the completion of reaction 1 and  $A_t$  is the  $\text{NO}_3$  absorbance at time  $t$ . The 662 nm temporal profile obtained after reaction 1 had gone to completion,  $t > 0.002$  s, was extrapolated to time zero, time of the laser pulse, to obtain the absorbance corresponding to the final concentration of  $\text{NO}_3$ ,  $A_\infty$ . The solid line in Figure 1 shows the linear least squares fit to the slowly decaying  $\text{NO}_3$  absorption signal at times greater than 0.002 s. The measured  $\text{NO}_3$  temporal profiles were fit to eq 4 using a linear least squares fitting routine to obtain  $k_1'$ ; such a fit is shown in Figure 2 using the data from Figure 1. As seen in Figure 2, the data obey eq 4 for at least three time constants. The obtained  $k_1'$  values were divided by the  $[\text{ClONO}_2]$  to calculate  $k_1$ .

The measured values of  $k_1$  and the experimental parameters used in their measurements are summarized in Table 1. At 298 K, the initial concentration of Cl,  $[\text{Cl}]_0$ , was varied over a factor of 20. As seen in Table 1, the measured values of  $k_1$  increased when  $[\text{Cl}]_0$  was close to  $[\text{ClONO}_2]$ . This was an indication of a secondary reaction(s), and only the values measured with a  $[\text{ClONO}_2]/[\text{Cl}]_0$  ratio greater than 34 were deemed correct and used in the derivation of the Arrhenius parameters. These data are labeled with an asterisk.

Even though reaction 1 is very fast, the reaction of Cl atoms with  $\text{NO}_3$ ,



can compete with reaction 1 if the concentration of  $\text{ClONO}_2$  is

TABLE 1: Summary of NO<sub>3</sub> Transient Absorption Rate Coefficient Measurements

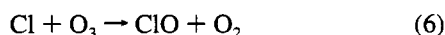
T (K)	[O <sub>3</sub> ] (10 <sup>14</sup> , molecule cm <sup>-3</sup> )	[Cl <sub>2</sub> ] (10 <sup>16</sup> , molecule cm <sup>-3</sup> )	ΔA <sub>253.7</sub>	[Cl] <sub>0</sub> (10 <sup>13</sup> , molecule cm <sup>-3</sup> )	[ClONO <sub>2</sub> ] (10 <sup>14</sup> , molecule cm <sup>-3</sup> )	[ClONO <sub>2</sub> ]/[Cl]	A <sub>∞</sub> (662)	k <sub>1</sub> <sup>a</sup> (10 <sup>-12</sup> , cm <sup>3</sup> molecule <sup>-1</sup> s <sup>-1</sup> )
298	6.11	3.88	0.0135	1.96	7.12	36.4	0.0401	10.3*
	5.14	3.53	0.0104	1.65	5.64	34.1	0.0287	10.0*
	4.23	4.03	0.0106	1.53	5.57	36.3	0.0302	9.24*
	4.16	4.04	0.0080	1.17	5.55	47.4	0.0224	9.32*
	4.16	4.04	0.0075	1.08	5.53	51.2	0.0224	9.32*
	3.88	4.07	0.0012	0.174	5.50	315.6	0.00309	8.85*
	3.88	4.07	0.00132	0.192	5.52	287.4	0.00382	9.11*
	5.27	3.19	0.0074	1.076	4.50	41.8	0.0194	10.2*
	6.05	3.06	0.00512	0.744	8.37	112.5	0.0155	9.19*
	5.72	4.07	0.0256	3.73	5.30	14.2	0.0594	11.2
	5.72	4.07	0.0184	2.67	5.31	19.9	0.0480	11.3
	2.51	3.57	0.00946	1.37	9.35	68.0	0.0285	10.0*
	4.27	3.58	0.109	15.9	6.09	3.83	0.133	15.8
	4.27	3.58	0.0891	13.0	6.11	4.70	0.123	14.5
	2.64	3.93	0.0186	2.70	3.21	11.9	0.0404	12.1
							average	9.56 ± 0.92
258	4.89	4.48	0.00494	0.719	4.68	64.9	0.0174	10.3
	4.89	4.48	0.00540	0.824	4.91	59.6	0.0169	10.6
	4.83	4.49	0.00757	1.10	4.69	42.6	0.0260	10.9
	4.83	4.49	0.00787	1.14	4.67	41.0	0.0247	10.7
	2.55	4.04	0.00619	0.900	4.68	52.0	0.0202	11.0
							average	10.7 ± 0.55
230	5.36	5.05	0.00761	1.11	5.12	46.2	0.0282	11.4
	5.36	5.05	0.00732	1.064	5.12	48.1	0.0265	11.9
	5.27	4.42	0.00692	1.01	4.934	49.0	0.0241	11.7
	5.27	4.42	0.00567	0.824	4.94	59.9	0.0214	11.3
							average	11.6 ± 0.55
200	5.86	5.08	0.00616	0.895	5.79	64.7	0.0245	13.1
	5.86	5.08	0.00683	0.992	5.78	58.3	0.0272	12.0
	2.91	4.12	0.00700	1.02	6.05	59.3	0.0284	12.2
	2.91	4.12	0.00636	0.924	6.04	65.4	0.0243	12.2
							average	12.4 ± 0.98

<sup>a</sup> \* indicates data used in average.

comparable to that of Cl. The rate coefficient for this reaction is  $k_5 = 2.4 \times 10^{-11} \text{ cm}^3 \text{ molecule}^{-1} \text{ s}^{-1}$ .<sup>9</sup> The occurrence of reaction 5 can be minimized by decreasing the initial Cl atom concentration to keep the  $[\text{ClONO}_2]/[\text{Cl}]_0$  ratio as large as possible. If this ratio is greater than 34, the loss of Cl atoms via reaction with NO<sub>3</sub> increases the measured value of  $k_1$  by less than 3%. Note that reaction 5 not only increases the rate of Cl atom loss but also suppresses the final value of the NO<sub>3</sub> produced; both factors increase the calculated value of  $k_1$ .

The values of the rate coefficient measured with  $[\text{ClONO}_2]/[\text{Cl}]_0$  ratios less than 34 are also given in the table to illustrate the effect of reaction 5 on the measured value of  $k_1$ . The measured value of  $k_1$  increased systematically as the  $[\text{ClONO}_2]/[\text{Cl}]_0$  ratio decreased. At all other temperatures,  $[\text{ClONO}_2]/[\text{Cl}]_0$  ratios greater than 40 were used to avoid this problem.

From the above discussions it is clear that knowledge of  $[\text{Cl}]_0$  is needed to ensure that the  $[\text{ClONO}_2]/[\text{Cl}]_0$  ratios are indeed acceptably high.  $[\text{Cl}]_0$  can be roughly estimated from the measured laser fluence and  $[\text{Cl}_2]$ . It can be determined more accurately as described in detail elsewhere.<sup>11</sup> Briefly, the amount of Cl<sub>2</sub> photolyzed was measured when ozone was added to the absorption cell to convert Cl to ClO and in the process destroy an equivalent amount of O<sub>3</sub> via the reaction



ClO formed in this reaction also absorbs at 253.7 nm. However, the change in the absorption at 253.7 nm was easily measurable even though the increase in absorption by the formation of ClO partially offsets the decrease due to the loss of O<sub>3</sub>. The difference between the absorption cross sections of ClO and O<sub>3</sub> is known accurately<sup>14</sup> and was used in these calculations.

**Cl Atom Resonance Fluorescence.** Figure 3 shows a typical decay profile of the chlorine atom signal. The Cl atom profiles

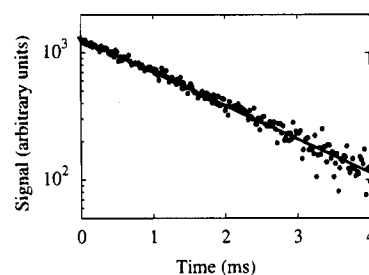
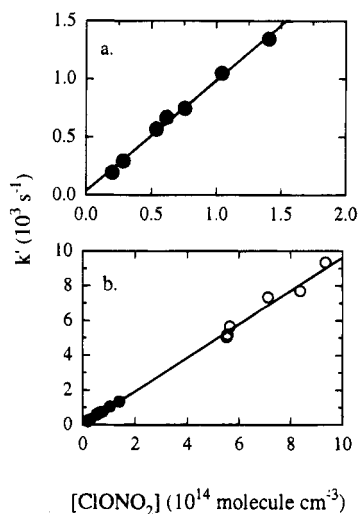


Figure 3. Typical temporal profile of the Cl atom resonance fluorescence signal following 355 nm laser photolysis of a Cl<sub>2</sub>/ClONO<sub>2</sub> mixture. The solid line shows the weighted least squares fit of the data to eq 7 used to obtain  $k'$ .

were strictly exponential over at least two lifetimes. The solid line in Figure 3 is the weighted least squares fit to the equation

$$\ln([\text{Cl}]_0/[\text{Cl}]_t) = (k_1[\text{ClONO}_2] + k_d)t = k't \quad (7)$$

whose slope yields the pseudo-first-order rate coefficient,  $k'$ , for the loss of Cl atoms. In the above equation,  $k_d$  is the first-order rate coefficient for the loss of Cl atoms in the absence of ClONO<sub>2</sub>. The first data point which was recorded during the photolysis laser pulse was not included in the fit. The temporal profile of Cl measured in the presence of an excess of ClONO<sub>2</sub> is determined by its (a) reaction with ClONO<sub>2</sub>, (b) reaction with impurities, and (c) diffusion out of the detection region. In this analysis we assume that the loss of Cl atoms in the absence of ClONO<sub>2</sub>, i.e., processes b and c, is first order in [Cl]. Indeed, the temporal profiles measured in the absence of ClONO<sub>2</sub> are exponential. Temporal profiles, such as that shown in Figure 3, were measured at various concentrations of ClONO<sub>2</sub>. The rate coefficient  $k_1$  was obtained from the slope of a  $k'$  vs  $[\text{ClONO}_2]$  plot, such as that shown in Figure 4. These



**Figure 4.** Plot of the first-order Cl atom loss rate coefficients at 298 K,  $k'$  ( $T=298$  K), vs  $[\text{ClONO}_2]$ . Data obtained using Cl atom resonance fluorescence (solid circles) are shown in part a. In part b, the data from the resonance fluorescence system (solid circles) and the transient  $\text{NO}_3$  absorption measurements (open circles) are shown. The solid line is the linear least squares fit to the data to yield  $k_1(T=298$  K).

measurements were carried out at ten temperatures between 195 and 354 K. The results from these studies, along with the conditions used for the measurements, are given in Table 2.

### Discussion

The major factors that influence the accuracy of the measured reaction rate coefficients in our two systems are (1) the uncertainties in the measured concentrations of the excess reagent,  $\text{ClONO}_2$ , (2) the precision with which the temporal profiles of Cl atoms or  $\text{NO}_3$  radicals could be measured, (3) the precision of the variation of  $k'$  with  $[\text{ClONO}_2]$ , (4) interferences from unrecognized secondary reactions influencing the measured temporal profiles, and (5) contributions of impurities to the measured temporal profiles. Each of these factors is discussed below.

The accuracy of the measured values of  $k_1$  was mostly limited by the accuracy of the concentration of  $\text{ClONO}_2$ . The  $\text{ClONO}_2$  concentrations are related to its UV absorption cross sections at the specific wavelengths employed for the measurements. The accuracy of the absorption cross sections of  $\text{ClONO}_2$  is discussed in our recent paper dealing with its measurements.<sup>4</sup> Uncertainty in the  $\text{ClONO}_2$  absorption cross section contributes a possible systematic error to the rate coefficients. Other factors such as the path lengths and pressure measurements are more accurate and contribute less than 2% to the uncertainty in the measured concentration. In the resonance fluorescence experiments, the concentrations were always measured at 298 K and then corrected for the temperature of the reactor. Thus the accuracy in the temperature dependence of the cross sections does not enter into estimating the accuracy of  $k_1$ . Also, in the resonance fluorescence experiments, we diluted the flow after the  $\text{ClONO}_2$  concentration was measured by UV absorption. This dilution procedure may contribute another 4% to the uncertainties in the concentration. In the long path laser absorption system,  $[\text{ClONO}_2]$  was measured in the reactor itself at the temperature of the experiment. The accuracy of the  $\text{ClONO}_2$  UV absorption cross sections at various temperatures is discussed elsewhere.<sup>4</sup> On the basis of these factors, we estimate the absolute uncertainty in the concentration of  $\text{ClONO}_2$  in our system to be better than 8% at the 95% confidence limit. This uncertainty is included in the uncertainties of  $k(298$  K) and the calculated A factor quoted in Table 3. The errors introduced via the thermal dissociation of  $\text{ClONO}_2$  and its contribution to the lowering of the  $\text{ClONO}_2$  concentration in the cell at higher temperatures are discussed later.

The precision of  $k'$  values determined from the temporal profiles and the plots of  $k'$  vs  $[\text{ClONO}_2]$  was in the range 5–8% and was explicitly determined in the data analysis. The errors in  $k'$  enter as weighting factors in the analysis of the  $k'$  vs  $[\text{ClONO}_2]$  data. The precision of these plots is included in the errors quoted below.

Interference from unrecognized secondary reactions is also a possible source of error. In these experiments, we varied various factors such as the ratio of  $[\text{ClONO}_2]/[\text{Cl}]_0$  and the

**TABLE 2: Experimental Conditions and the Measured Values of  $k_1$  Using the Pulse Photolysis–Resonance Fluorescence System**

$T$ (K)	$[\text{Cl}]_0$ ( $10^{11}$ molecule $\text{cm}^{-3}$ )	$[\text{ClONO}_2]$ ( $10^{13}$ molecule $\text{cm}^{-3}$ )	pressure (Torr)	$k_1 \pm 2(\sigma)^a$
195	4.3	1.8–8.97	55	$12.4 \pm 0.42$
196	10.1	3.17–12.6	101 <sup>d</sup>	$12.2 \pm 0.4$
			average for 195 K	$12.3 \pm 0.5$
213	5.2	1.9–9.7 <sup>b</sup>	55	$11.6 \pm 0.5$
233	6.2	2.1–17.3 <sup>c</sup>	56	$10.4 \pm 0.81$
233	6.6	2.43–16.8 <sup>c</sup>	56	$10.9 \pm 0.76$
			average for 233 K	$10.7 \pm 0.8$
252	5.9	1.10–11.4	55	$10.3 \pm 0.4$
271	8.5	1.76–9.74 <sup>c</sup>	25	$10.5 \pm 0.9$
297	5.4	2.64–12.1 <sup>c</sup>	60	$9.35 \pm 0.57$
298	5.5	1.58–10.1	58	$9.17 \pm 0.44$
298	1.8	1.55–8.37	55	$9.78 \pm 0.26$
299	8.3	1.54–13.1	48	$9.74 \pm 0.49$
299	8.3	2.01–14.1	50 <sup>e</sup>	$9.52 \pm 0.62$
299	15	0.93–14.9	103 <sup>e</sup>	$9.46 \pm 0.43$
299	7.4	1.5–9.8	70 <sup>e,f</sup>	$10.1 \pm 1.2$
			average for 298 K	$9.59 \pm 0.62$
312	5.8	1.49–11.4	57	$9.71 \pm 0.19$
324	7.2	2.29–16.9 <sup>c</sup>	56	$9.72 \pm 0.20$
336	6.5	1.25–6.5	57	$9.90 \pm 0.40$
354	10.7	0.92–7.3	58	$9.18 \pm 0.50$
354	9.2	0.96–6.5	28 <sup>d</sup>	$9.36 \pm 0.20$
			average for 354 K	$9.27 \pm 0.50$

<sup>a</sup>  $10^{-12}$   $\text{cm}^3$  molecule<sup>-1</sup> s<sup>-1</sup>. Quoted is precision at the 95% confidence level. <sup>b</sup> In some experiments,  $[\text{ClONO}_2]$  was directly measured via UV absorption. <sup>c</sup>  $[\text{ClONO}_2]$  was directly measured via UV absorption. <sup>d</sup> The velocity of gas flow was increased by a factor of  $\sim 3$ . <sup>e</sup> 2–5 Torr of  $\text{CF}_4$  was added to quench  $\text{Cl}(^2\text{P}_{1/2})$ . <sup>f</sup> The velocity of gas flow was increased by a factor of  $\sim 1.5$ .

TABLE 3: Comparison of the Values of  $k_1$  Measured in This Study with Those from Previous Studies and Evaluations

$k(298\text{ K})^a$	$A^a$	$E/R$ (K)	$T$ range (K)	method <sup>b</sup>	ref/comments
$1.04 \pm 0.16^c$	0.63	-150	219–298	LP-RF	7
$1.27 \pm 0.24^d$	0.73	-165	220–298	FP-RF	8
$0.959 \pm 0.098$	$0.61 \pm 0.04$	$-140 \pm 30$	195–298	LP-RF	this work
	$0.65 \pm 0.05$	$-120 \pm 30$	195–354	LP-RF	this work
$0.96 \pm 0.12$	$0.60 \pm 0.04$	$-140 \pm 30$	195–298	LP-LPLA	this work
	$0.60 \pm 0.04$	$-140 \pm 30$	195–298	LP-RF and LP-LPLA	this work
1.2	0.68	$-160 \pm 200$			9 and 10
$0.96^e$	0.60	$-140 \pm 40$	195–298		our data in evaluation format <sup>f</sup>
$1.0^g$	0.65	$-135 \pm 50$	195–298		recommended <sup>g</sup>

<sup>a</sup> In units of  $10^{-11} \text{ cm}^3 \text{ molecule}^{-1} \text{ s}^{-1}$ . <sup>b</sup> LP, laser photolysis; RF, resonance fluorescence; FP, flash photolysis (broad band); LPLA, long path laser absorption. <sup>c</sup> Margitan quoted that his overall uncertainty in the values of  $k(298 \text{ K})$  was 15%. He did not specifically quote error bars for the Arrhenius parameters, and hence, they are not included in the table. <sup>d</sup> The uncertainty of  $k(298 \text{ K})$  is that quoted by Kurylo *et al.* They did not specifically quote error bars for the Arrhenius parameters, and hence, they are not included in the table. <sup>e</sup> The uncertainty in  $k(298 \text{ K})$  is  $f(298 \text{ K}) = 1.10$ . <sup>f</sup> Error of  $k(T)$  at temperature  $T$  is given by  $f(T) = f(298 \text{ K})\Delta(E/R)|1/T - 1/298|$ . The uncertainty in  $E/R$  has been increased to reflect that all uncertainties are now included in  $k(298 \text{ K})$  and  $E/R$ . <sup>g</sup> Obtained using the data of Margitan and this study in the temperature range 195–298 K.

values of  $[\text{Cl}]_0$  and  $[\text{ClONO}_2]$ . The range of these variations is shown in Tables 1 and 2. None of these variations changed the measured value of the rate coefficient, except the ratio of  $[\text{ClONO}_2]/[\text{Cl}]_0$  in the long path absorption experiments, which was discussed earlier.

It is known that small amounts, 2%, of spin-orbit excited Cl atoms,  $\text{Cl}(^2\text{P}_{1/2})$ , are produced in the 355 nm photolysis of  $\text{Cl}_2$ .<sup>15,16</sup>  $\text{Cl}(^2\text{P}_{1/2})$  is also produced in  $\text{ClONO}_2$  photolysis ( $\sim 30\%$  at 308 nm).<sup>17</sup> However, the present measurements used 355 nm photolysis where the  $\text{Cl}(^2\text{P}_{1/2})$  yield has not been measured and the photolysis of  $\text{ClONO}_2$  was small compared to that of  $\text{Cl}_2$ . It is possible that  $\text{Cl}(^2\text{P}_{1/2})$  reacts at a different rate than  $\text{Cl}(^2\text{P}_{3/2})$ . Further, the detection sensitivity of our apparatus to  $\text{Cl}(^2\text{P}_{1/2})$  and  $\text{Cl}(^2\text{P}_{3/2})$  is undefined and is likely to vary with the conditions of the resonance lamp. Lastly, the rate coefficient for the reaction of  $\text{Cl}(^2\text{P}_{3/2})$  is the quantity of interest for atmospheric purposes. Therefore, it is necessary to quench spin-orbit excited Cl atoms to the ground state such that the ratio of the spin-orbit excited to the ground state is maintained at the thermal (Boltzman) distribution. The rate coefficient for the quenching of  $\text{Cl}(^2\text{P}_{1/2})$  by He is  $6 \times 10^{-14} \text{ cm}^3 \text{ molecule}^{-1} \text{ s}^{-1}$ .<sup>17</sup> Thus, all the  $\text{Cl}(^2\text{P}_{1/2})$  should be removed within  $\sim 100 \mu\text{s}$  after generation in our resonance fluorescence system and much faster in our long path absorption system, and the temporal profiles measured at longer times would not be affected by the presence of  $\text{Cl}(^2\text{P}_{1/2})$ . To check if  $\text{Cl}(^2\text{P}_{1/2})$  could indeed be affecting our measured values, we added 2–5 Torr of  $\text{CF}_4$  to the system (see Table 2). The rate coefficient for the quenching of  $\text{Cl}(^2\text{P}_{1/2})$  by  $\text{CF}_4$  is  $\sim 2 \times 10^{-11} \text{ cm}^3 \text{ molecule}^{-1} \text{ s}^{-1}$ , such that all the  $\text{Cl}(^2\text{P}_{1/2})$  will be quenched to the ground state within 2  $\mu\text{s}$ . The measured rate coefficients were the same as in the absence of  $\text{CF}_4$ , thus showing that our measured rate coefficients are not affected by the reactions of  $\text{Cl}(^2\text{P}_{1/2})$  (see Table 2).

The chlorine atom signal was also observed when chlorine nitrate was photolyzed without adding  $\text{Cl}_2$ . The signal results from photolysis of both  $\text{ClONO}_2$  and the  $\text{Cl}_2$  impurity. The Cl atom signal was very small but yielded a rate coefficient equal to  $k_1$  obtained when  $\text{Cl}_2$  was added to the photolysis mixture. The possibility of Cl atom loss via reaction with  $\text{NO}_3$ , produced from  $\text{ClONO}_2$  photolysis, was considered. Use of  $[\text{ClONO}_2]/[\text{Cl}]_0$  ratios greater than 40 minimized the secondary reactions of Cl atoms with  $\text{NO}_3$ .

The presence of species, other than  $\text{ClONO}_2$ , that can react with Cl atoms in our system can contribute to errors in the measured values of  $k_1$ . Such species may be formed following reaction 1 and accumulate in the reactor if they are not rapidly swept away. To check for buildup of such species, the flow velocity through the resonance fluorescence reactor was varied between 13 and 44  $\text{cm s}^{-1}$ , with no change in the measured

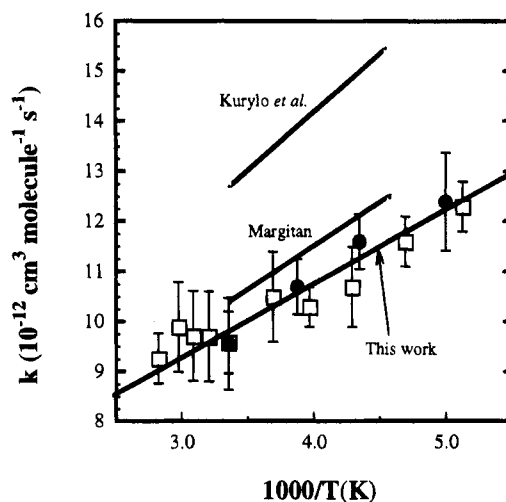


Figure 5. Arrhenius plot for reaction 1: This work (solid circles, transient  $\text{NO}_3$  absorption; open squares, Cl atom resonance fluorescence). The solid lines are the Arrhenius lines. The error bars shown are the  $2\sigma$  values and include estimated systematic errors.

value of the rate constant. Even at 354 K, variations in the flow velocity did not change the measured value of  $k_1$ . Similarly, changes in the flow velocity in the long path absorption experiments did not change the rate constants. Therefore, any systematic errors due to reaction products or thermal decomposition products are negligible. The levels of  $\text{OClO}$  and  $\text{Cl}_2\text{O}$  impurities in our  $\text{ClONO}_2$  samples are too small to contribute to the photolytic production of Cl atoms. The presence of small amounts of  $\text{Cl}_2$  does not interfere with the measurement of  $\text{ClONO}_2$  concentration via UV absorption. It also does not lead to significant Cl atom production. Also, the levels of  $\text{Cl}_2\text{O}$ ,  $\text{OClO}$ , and  $\text{NO}_2$  are too small to contribute to the loss of Cl atoms and thus affect the measured value of  $k_1$ . Thus, we are confident that impurities did not affect our measured rate coefficients.

We employed two different experimental methods to measure  $k_1$ . Figure 4 shows the variation of  $k'$  with  $\text{ClONO}_2$  from both the resonance fluorescence and the long path absorption systems on the same plot. It is clear that one line fits both sets of data. The obtained values are independent of the method, and hence, it is very unlikely that our rate coefficients have some unrecognized systematic error.

The rate coefficients over the temperature range 200–354 K from the two different experimental methods are shown in Figure 5. The two data sets are in excellent agreement over the entire temperature range. Also shown in the figure are the rate coefficient data reported by Margitan<sup>7</sup> and Kurylo.<sup>8</sup> Table

3 also lists our data along with those from previous studies. The Arrhenius expression shown in Table 3 was derived using our data in the temperature range 200–298 K. Also shown in the table are the values of our rate coefficients in the form commonly used in evaluations.<sup>9,10</sup>

The Arrhenius parameters obtained from this study are in good agreement with that reported by Margitan<sup>7</sup> but are lower than that reported by Kurylo *et al.*<sup>8</sup> However, the discrepancy between our measurements and those of Kurylo *et al.* is only just outside their quoted error limit of  $\pm 20\%$ . Therefore, we recommend an expression obtained by using our results and those of Margitan,<sup>7</sup>  $k_1(T) = 6.5 \times 10^{-12} \exp(135/T) \text{ cm}^3 \text{ molecule}^{-1} \text{ s}^{-1}$ , for use in atmospheric model calculations, which again is given in Table 3. The quoted error bounds overlap with Kurylo *et al.*'s results.

The rate coefficients measured using the resonance fluorescence method at temperatures greater than 298 K are slightly higher than that predicted by the Arrhenius expression derived from only the lower temperature data. If all the data between 195 and 354 K are used in the analysis, we obtain  $k_1 = (6.5 \pm 0.5) \times 10^{-12} \exp[(130 \pm 20)/T] \text{ cm}^3 \text{ molecule}^{-1} \text{ s}^{-1}$ . Within the quoted uncertainties, these two Arrhenius expressions are the same. Yet, for atmospheric purposes, we prefer to quote the expression obtained using only the lower temperature values.

We are the first to report values of  $k_1$  at  $T > 298 \text{ K}$ . One possible source of error at high temperatures is the thermal decomposition of  $\text{ClONO}_2$ . The end products of the thermal decomposition are  $\text{NO}_2$  and  $\text{Cl}_2$ . We can calculate the extent of thermal decomposition due to gas phase processes using known rate coefficients.<sup>9</sup> On the basis of these calculations, it is clear that gas phase thermal decomposition is not a problem in our system at temperatures below  $\sim 390 \text{ K}$ . If thermal decomposition occurred, it will eventually (in the time it takes for the gas mixture to get to the reaction zone in the cell) lead to  $\text{Cl}_2$  and  $\text{NO}_2$ . The reaction of  $\text{Cl}$  with  $\text{NO}_2$  is much slower than that with  $\text{ClONO}_2$ . Therefore, if thermal decomposition depletes the  $\text{ClONO}_2$  concentration in the reactor, the measured rate constant would be lower. Indeed, the rate coefficient measured at 390 K was  $\sim 3 \times 10^{-12} \text{ cm}^3 \text{ molecule}^{-1} \text{ s}^{-1}$ , a factor of  $\sim 3$  lower than that at 298 K. This drop in the measured value is consistent with the expected decomposition. Further, in our studies of  $\text{O}(^3\text{P})$  atom reactions with  $\text{ClONO}_2$ <sup>18</sup> at  $T > 298 \text{ K}$ , the rate coefficient increased due to the formation of  $\text{NO}_2$ , which reacts much faster with  $\text{O}(^3\text{P})$  than does  $\text{ClONO}_2$ . On the basis of the measured increases in the rate constant for the  $\text{O} + \text{ClONO}_2$  reaction, we are confident that thermal decomposition of  $\text{ClONO}_2$  was quite small at 354 K and does not contribute to the measured values of  $k_1$ . Lastly, variation in the flow rate of the gas through the reactor (i.e., change in the residence time available for thermal dissociation) did not affect the measured rate coefficient at 354 K. Therefore, we believe that thermal decomposition of  $\text{ClONO}_2$  is not a significant contributor to the errors in the reported values of  $k_1$  at  $T < 354 \text{ K}$ .

The reaction of  $\text{Cl}$  with  $\text{ClONO}_2$  has many possible reaction pathways leading to different products:

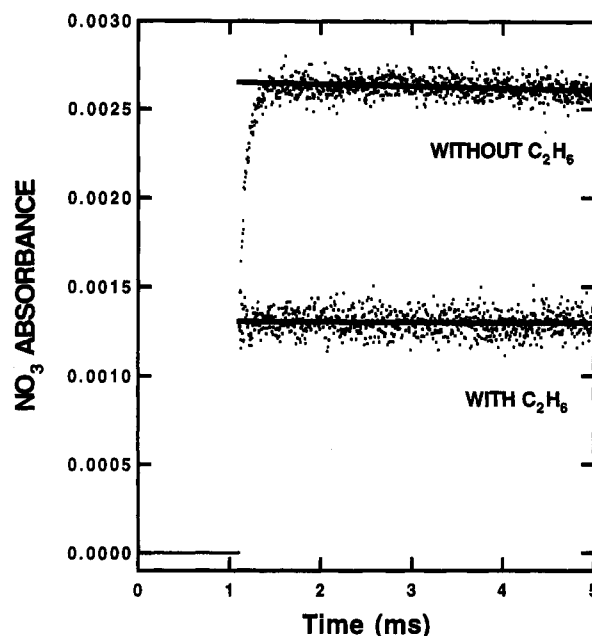
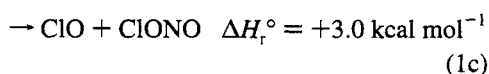
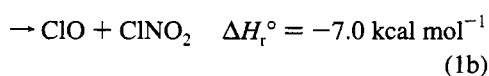
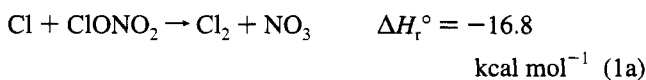
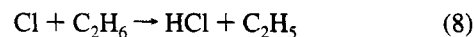


**Figure 6.** Temporal profiles of  $\text{NO}_3$  absorption following the photolysis of  $\text{ClONO}_2$  at 308 nm, where the quantum yield of  $\text{Cl}$  is the same as that for  $\text{NO}_3$ . The upper curve was measured in the absence of  $\text{C}_2\text{H}_6$  while the lower curve was obtained in the presence of  $\text{C}_2\text{H}_6$ . The  $[\text{ClONO}_2]$  and laser fluence are the same for both experiments.

Other thermodynamically allowed channels include production of  $\text{Cl}_2\text{O} + \text{NO}_2$  and  $\text{Cl}_2 + \text{O}_2 + \text{NO}$ , which are discounted as unlikely for such a fast reaction. We carried out a few experiments to identify the products of reaction 1 at 298 K.

We photolyzed  $\text{ClONO}_2$  at 308 nm (XeCl excimer laser) and observed the temporal profiles of  $\text{NO}_3$ . Even though the products of  $\text{ClONO}_2$  photolysis are currently a matter of controversy, work in our laboratory suggests that the quantum yields for  $\text{Cl}$  and  $\text{NO}_3$  are equal at 308 nm.<sup>19</sup> We know from these experiments that the yields of  $\text{O}$  atoms at 308 nm are very small, which rules out the production of  $\text{Cl} + \text{NO}_2 + \text{O}$  as products. Figure 6 shows the temporal profile of absorption due to  $\text{NO}_3$  measured in back to back experiments where  $\text{ClONO}_2$  was photolyzed at 308 nm in the presence and the absence of excess  $\text{C}_2\text{H}_6$ .  $\text{C}_2\text{H}_6$  scavenges  $\text{Cl}$  atoms via the reaction



such that the subsequent reaction of  $\text{Cl}$  atoms with  $\text{ClONO}_2$  is suppressed. To ensure that the reaction of  $\text{C}_2\text{H}_5$  radical with  $\text{ClONO}_2$  would not interfere,  $\text{O}_2$  was added to scavenge the  $\text{C}_2\text{H}_5$  radical. It is clear from the results shown in Figure 6 that the concentration of  $\text{NO}_3$  measured when the  $\text{Cl}$  atom reaction with  $\text{ClONO}_2$  is suppressed is 50% of that when it is allowed to react with  $\text{ClONO}_2$ . On the basis of such experiments, we conclude that at 298 K greater than 95% of reaction 1 leads to  $\text{Cl}_2$  and  $\text{NO}_3$ .

Channel 1c is a direct  $\text{O}$  atom abstraction and is endothermic by  $3 \text{ kcal mol}^{-1}$ . Therefore, it could become important at higher temperatures. For example, if the rate coefficient for channel 1c has an  $A$  factor of  $3 \times 10^{-11}$  and an activation energy of  $3 \text{ kcal mol}^{-1}$ , it could contribute  $\sim 5\%$  to the measured value of  $k_1$  at 354 K, the highest temperature for which  $k_1$  is reported. Its contribution to  $k_1$  would be at most 2% at 298 K. Channel 1b is unlikely to be important because of the large amount of rearrangement necessary for this reaction. Therefore, we believe that the sole products of reaction 1 at the low temperatures of the atmosphere are  $\text{Cl}_2$  and  $\text{NO}_3$ . Measurements of  $k_1$  at higher

temperatures without thermally dissociating ClONO<sub>2</sub> and/or the identification of any minor products in reaction 1 would establish if channels 1b and 1c are of importance at high temperatures.

**Acknowledgment.** We thank L. Greg Huey for the CIMS analyses of the ClONO<sub>2</sub> samples. This work was funded in part from the National Aeronautic and Space Administration's Mission to Planet Earth Program. LG thanks the NASA Global Change Research Program for a doctoral fellowship.

### References and Notes

- (1) *Scientific Assessment of Ozone Depletion: 1991*; Global Ozone Research and Monitoring Project, World Meteorological Organization: Geneva, Switzerland, 1992; No. 25.
- (2) Webster, C. R.; May, R. D.; Toohey, D. W.; Avallone, L. M.; Anderson, J. G.; Newman, P.; Laitt, L.; Schoeberl, M. R.; Elkins, J. W.; Chan, K. R. *Science* **1993**, *261*, 1130.
- (3) Solomon, S. *Rev. Geophys.* **1988**, *26*, 131.
- (4) Burkholder, J. B.; Talukdar, R. K.; Ravishankara, A. R. *Geophys. Res. Lett.* **1994**, *21*, 585.
- (5) Ravishankara, A. R.; Davis, D. D.; Smith, G.; Tesi, G.; Spencer, J. *Geophys. Res. Lett.* **1977**, *4*, 7.
- (6) Kurylo, M. J.; Manning, R. G. *Chem. Phys. Lett.* **1977**, *48*, 279.
- (7) Margitan, J. J. *J. Phys. Chem.* **1983**, *87*, 674.
- (8) Kurylo, M. J.; Knable, G. L.; Murphy, J. L. *Chem. Phys. Lett.* **1983**, *95*, 9.

- (9) DeMore, W. B.; Sander, S. P.; Golden, D. M.; Hampson, R. F.; Kurylo, M. J.; Howard, C. J.; Ravishankara, A. R.; Kolb, C. E.; Molina, M. J. *Chemical Kinetics and Photochemical Data for use in Stratospheric Modeling*; Jet Propulsion Laboratory: Pasadena, CA, 1994; JPL Pub. No. 94-26.
  - (10) Atkinson, R.; Baulch, D. L.; Cox, R. A.; Hampson, R. F.; Kerr, J. A.; Troe, J. *J. Phys. Chem. Ref. Data* **1992**, *21*, 1125.
  - (11) Yokelson, R. J.; Burkholder, J. B.; Fox, R. W.; Talukdar, R. K.; Ravishankara, A. R. *J. Phys. Chem.* **1994**, *98*, 13144.
  - (12) Warren, R. F.; Ravishankara, A. R. *Int. J. Chem. Kinet.* **1993**, *25*, 833.
  - (13) Gierczak, T.; Goldfarb, L.; Sueper, D.; Ravishankara, A. R. *Int. J. Chem. Kinet.* **1994**, *26*, 719.
  - (14) Trolier, M.; Mauldin, R. L., III; Ravishankara, A. R. *J. Phys. Chem.* **1990**, *94*, 4896.
  - (15) Busch, G. E.; Mahoney, R. T.; Morse, R. I.; Wilson, K. R. *J. Chem. Phys.* **1969**, *51*, 449.
  - (16) Diesen, R. W.; Wahr, J. C.; Adler, S. E. *J. Chem. Phys.* **1971**, *55*, 2812.
  - (17) Tyndall, G. S.; Kegley-Owen, C. S.; Orlando, J. J. *J. Chem. Soc., Faraday Trans.*, submitted for publication (1995) and references therein.
  - (18) Goldfarb, L.; Gilles, M. K.; Ravishankara, A. R. Manuscript in preparation (1995).
  - (19) Yokelson, R. L.; Burkholder, J. B.; Ravishankara, A. R. Manuscript in preparation (1995).
- JP951074D